Indian Journal of Experimental Biology
Vol. 63, August 2025, pp. 665-672
DOI: 10.56042/ijeb.v63i08.17447

Osteomodulin silencing alleviates renal podocyte injury in membranous nephropathy by inhibiting pyroptosis

Daoyuan Lv[1,2], Yuqing Su[1,2], Laping Chu[1,2], Yuan Du[1,2], Neng Bao[1,2], Yanlie Zheng[3]* & Yafen Yu[1,2]*

[1]Department of Nephrology, Affiliated Hospital of Jiangnan University, Wuxi, China

[2]Wuxi School of Medicine, Jiangnan University, Wuxi, China

[3]Department of Infectious Disease, General Hospital of Southern Theater Command, Guangzhou, China

Received 25 February 2025; revised 02 May 2025

Membranous nephropathy (MN) is an autoimmune disorder primarily characterized by renal podocyte injury. The emerging role of pyroptosis, a novel form of regulated cell death, in the pathogenesis of podocyte damage in MN underscores the need to identify additional regulators and inhibitors of pyroptosis to optimize MN treatment. This study examined osteomodulin (OMD) as a potential regulator of pyroptosis in MN using a passive Heymann nephritis (PHN) rat model. OMD silencing in PHN rats resulted in an alleviation of nephrotic syndrome, as evidenced by reductions in 24-h urine protein and low-density lipoprotein levels, and increased albumin levels. Additionally, OMD silencing mitigated podocyte injury, as indicated by the restoration of podocyte foot process architecture, enhanced expression and normalization of Nephrin and Podocin, and reduced Desmin expression in glomeruli. Mechanistically, OMD silencing led to the inhibition of renal p38 MAPK activation and pyroptosis, demonstrated by decreased expression of intrarenal p-p38 MAPK (Thr180/Tyr182) and key pyroptosis markers, including NLRP3, ASC, Caspase-1, Caspase-1 p20, IL-1β, IL-18, GSDMD, and GSDMD-N, as well as lowered serum levels of IL-1β and IL-18. In conclusion, this study suggests that OMD silencing attenuates renal podocyte injury in MN through inhibiting pyroptosis, highlighting a promising new therapeutic approach for MN.

Keywords: Osteomodulin, Membranous nephropathy, Renal injury, Pyroptosis

Membranous nephropathy (MN) is an autoimmune disorder primarily affecting glomeruli, representing a leading cause of nephrotic syndrome and progression to end-stage renal disease (ESRD)[1,2]. MN is characterized by significant structural and functional impairment of renal podocytes, accompanied by subepithelial immune deposits and complement activation[2,3]. Therefore, elucidating the mechanisms underlying podocyte injury is essential for advancing MN treatment, which remains limited.

Pyroptosis, a pro-inflammatory form of regulated cell death, is typically induced by inflammasomes like NLRP3 and mediated by gasdermin proteins, particularly gasdermin D (GSDMD)[4,5]. Recent research has underscored the critical role of podocyte pyroptosis in the pathogenesis of MN[6-8], highlighting the potential of targeting key regulators and inhibitors of pyroptosis as promising therapeutic strategies.

*Correspondence:
Phone: +86 15951580601
E-mail: yafenyu@163.com

Osteomodulin (OMD), a small leucine-rich repeat proteoglycan within the extracellular matrix, was initially identified for its role in osteoblast differentiation and mineralization but has since been implicated in broader biological processes, including cell proliferation, migration, and apoptosis[9-12]. Among its regulatory functions, OMD influences the p38 mitogen-activated protein kinase (MAPK) signaling pathway, a crucial node in various biological effects[11,13], with recent evidence suggesting that p38 MAPK also plays a significant role in the regulation of pyroptosis[14,15]. Based on this, we hypothesized that OMD may contribute to renal podocyte injury in MN through its regulation of pyroptosis. In the passive Heymann nephritis (PHN) rat model, anti-Fx1A antibodies derived from rat renal tubular brush border glycoproteins bind podocyte antigens, forming subepithelial immune complexes that activate complement and drive podocyte injury and proteinuria, thus faithfully recapitulating the pathophysiological characteristics of human MN[16,17]. This study aims to validate the role of OMD-mediated pyroptosis in MN pathogenesis using the PHN model.

Materials and Methods

Animals

Female Sprague–Dawley (SD) rats, weighing between 150-180 g, were obtained from Vital River Laboratory Animal Technology Co. Ltd. (Beijing, China). The rats were housed in the SPF environment of the Laboratory Animal Center at Wuxi School of Medicine, Jiangnan University, with unrestricted access to standard chow and water. The study's animal experimental protocols received approval from the Experimental Animal Ethics Committee of Jiangnan University (Approval number: JN.No20231215S0400801-612).

Model establishment

Rabbit anti-Fx1A serum was prepared following Dr. Salant's protocol[18]. Briefly, the Fx1A antigen was extracted from SD rat kidneys *via* sieving and ultracentrifugation. Rabbits were immunized with Fx1A antigen emulsified in complete Freund's adjuvant at least four times, and the resulting anti-Fx1A serum was collected by centrifuging peripheral blood. The antibody concentrations were confirmed by assessing the immunofluorescence intensity of the brush border of the rat's proximal renal tubular epithelial cells. To induce the PHN model, rats received intraperitoneal injections of anti-Fx1A antiserum in volumes of 2 mL and 1 mL at 1-h intervals. Control rats received similar injections with normal rabbit serum to establish the normal control (NC) group.

Treatment, grouping, and specimen collections

OMD siRNA with 2'-O-methyl and cholesteryl modifications was purchased from Hippo Biotechnology (Huzhou, China), with the sense sequence (5'-3') GGCACUUCUGAUUCAGUUAAA. The siRNA was dissolved in normal saline and administered intravenously at a concentration of 1 nmol/g throughout the observation period after model establishment. The rats were randomly assigned to four groups: NC, OMD-siRNA (si-OMD), PHN, and PHN+OMD-siRNA (PHN+si-OMD). Rats were euthanized on day 15 post-modeling, a timepoint selected based on Dr. Salant's protocol and experimental validation of typical renal injury in MN[18]. Body weight, serum, 24-h urine, and kidneys were collected using a weighing scale, angular venipuncture, metabolism cages, and laparotomy, respectively. Rats that died during the experiment were excluded; 32 rats in total, 8 per group, were included in the final analysis.

Urinary protein and blood biochemical tests

Urinary protein concentration was measured using a Bradford protein assay kit (P0006, Beyotime Biotechnology, Shanghai, China), and 24-h urine protein (24 h-UPro) was calculated from urine volume. Serum albumin (ALB), total cholesterol (T-CHOL), triglycerides (TG), high-density lipoprotein (HDL), low-density lipoprotein (LDL), serum creatinine (SCr), and blood urea nitrogen (BUN) were analyzed using an automated biochemical analyzer (AU5800, Beckman Coulter, Inc., Indianapolis, USA).

Transmission electron microscopy (TEM)

Granules (1 mm^3) from the fresh renal cortex were fixed in 2.5% glutaraldehyde at 4°C overnight, followed by post-fixation with 1% osmium tetroxide at room temperature (RT) for 1-h. Ultrathin sections, 70 nm-thick, were stained with uranyl acetate and lead citrate. The renal tissue ultrastructure was then examined, and representative photomicrographs were captured using an electron microscope (H-7500, Hitachi, Ltd., Tokyo, Japan). The average podocyte foot process width was calculated using the formula $(\pi/4) \times (\Sigma$ glomerular basement membrane length/Σ number of foot processes) with Digital Micrograph software (Gatan, Inc., Pleasanton, USA)[19].

Immunohistochemistry

For immunohistochemical staining, 2.5 μm-thick paraffin sections of the renal cortex were deparaffinized, rehydrated, subjected to antigen retrieval, blocked with 10% calf serum, and incubated with Desmin antibody (16520-1-AP, 1:200 dilution, Proteintech Group Inc., Rosemont, USA) at RT overnight. The sections were then incubated with HRP-conjugated secondary antibodies (RQ7025, Quanhui Imp & Exp Int'l Co. Ltd., Zhuhai, China) at RT for 30 min, counterstained with hematoxylin, and sealed with neutral balsam. The stained tissues were observed, and representative micrographs were captured using a light microscope (Eclipse 80i, Nikon Instruments Inc., Tokyo, Japan). Three glomeruli from each section were randomly selected for semiquantitative analysis using Image-Pro Plus 6.0 software (Media Cybernetics, Rockville, USA). The integrated optical density (IOD) and area of each glomerulus were measured, and the average IOD/area of all three glomeruli in each section was used to quantify Desmin levels in the samples.

Immunofluorescence

For immunofluorescence staining, 5 μm-thick frozen sections of the renal cortex were blocked with 10% calf serum and incubated overnight at RT with Nephrin (DF7501, 1:100 dilution, Affinity Biosciences Ltd., Changzhou, China) and Podocin antibodies (20384-1-AP, 1:500 dilution, Proteintech Group). The sections were then incubated with FITC-labeled secondary antibodies (A0562, 1:200 dilution, Beyotime Biotechnology) at RT for 40 min. The stained tissues were observed, and representative images were captured using confocal microscopy (LSM710, Carl Zeiss Meditec AG, Oberkochen, Germany).

Western blotting

Total proteins from the fresh renal cortex were extracted using the T-PER™ Tissue Protein Extraction Reagent (78510, Thermo Fisher Scientific Inc., Waltham, USA) and quantified with the Enhanced BCA Protein Assay Kit (P0010, Beyotime Biotechnology). Equal amounts of protein were mixed with loading buffer, denatured by boiling, and subsequently separated *via* SDS-PAGE. The proteins were then transferred onto PVDF membranes and incubated overnight at 4°C with the following primary antibodies: OMD (bs-19642R, 1:500 dilution, BIOSYNTHESIS BIOTECHNOLOGY CO. LTD., Beijing, China), p38 MAPK (9212, 1:1000 dilution, Cell Signaling Technology, Inc., Danvers, USA), p-p38 MAPK (Thr180/Tyr182) (9211, 1:1000 dilution, Cell Signaling Technology, Inc.), NLRP3 (DF7438, 1:1000 dilution, Affinity Biosciences Ltd.), ASC (DF6304, 1:1000 dilution, Affinity Biosciences Ltd.), Caspase-1 (3866, 1:1000 dilution, Cell Signaling Technology, Inc.), IL-1β (12242, 1:1000 dilution, Cell Signaling Technology, Inc.), IL-18 (DF6252, 1:1000 dilution, Affinity Biosciences Ltd.), GSDMD (DF12275, 1:1500 dilution, Affinity Biosciences Ltd., Changzhou, China), GSDMD-N (DF13758, 1:1000 dilution, Affinity Biosciences Ltd.), and GAPDH (CW0100M, 1:3000 dilution, Cwbio IT Group, Taizhou, China). Following primary antibody incubation, membranes were incubated with HRP-conjugated secondary antibodies (Beyotime Biotechnology, A0216/A0208, 1:1000 dilution) at RT for 2-h. Protein visualization was performed using an Enhanced Chemiluminescent Kit (NcmECL Ultra, New Cell & Molecular Biotech Co. Ltd., P10200) and captured with an automatic chemiluminescence/ fluorescence image analysis system (5200 Multi, Tanon Science & Technology Co. Ltd., Shanghai, China). The IOD of each protein band was quantified using Image-Pro Plus 6.0 software, with the IOD ratio relative to GAPDH serving as the measure of protein expression levels.

ELISA

Serum IL-1β and IL-18 levels were quantified using rat IL-1β and IL-18 ELISA kits (EK0393 and EK0592, Boster Biological Technology Co. Ltd., Wuhan, China), according to the manufacturer′s protocols.

Statistical analysis

All experiments were conducted at least three times. Data analysis was performed using SPSS 20.0 software (IBM Corporation, Armonk, USA). Results are expressed as means ± standard deviations (SDs). Group differences were analyzed *via* analysis of variance (ANOVA) with the least significant difference (LSD) test (for equal variances) or the Welch test with Dunnett's T3 test (for unequal variances). Statistical significance was defined as $P < 0.05$.

Results

OMD silencing alleviated nephrotic syndrome in PHN rats

The effects of OMD silencing on the clinical manifestations of PHN rats were initially examined, as detailed in Table 1. PHN rats exhibited characteristic features of nephrotic syndrome, including elevated 24 h-UPro, T-CHOL, TG, HDL, and LDL levels, along with reduced ALB. Additionally, renal function impairment was evident through increased SCr and BUN levels. OMD silencing alleviated nephrotic syndrome of PHN rats, as demonstrated by reductions in 24 h-UPro and LDL levels, and an increase in ALB in the PHN+si-OMD group. Moreover, OMD silencing contributed to the preservation of renal function, as indicated by decreased SCr and BUN levels in the si-OMD-treated PHN group. Notably, no significant differences in 24 h-UPro, ALB, T-CHOL, TG, HDL, LDL, SCr, or BUN levels were observed between the NC and si-OMD groups, indicating that OMD silencing did not adversely affect the physiological status of normal kidneys. The safety of OMD silencing was further supported by the absence of significant differences in body weight among the groups. Collectively, these findings suggest that OMD silencing effectively alleviates nephrotic syndrome in PHN rats.

Table 1 — Clinical manifestations of all the rats in each group

Groups	Body weight (g)	24 h-UPro (mg)	ALB (g/L)	T-CHOL (mmol/L)	TG (mmol/L)	HDL (mmol/L)	LDL (mmol/L)	SCr (mg/dL)	BUN (mg/dL)
NC	192.90 ± 10.22	5.04 ± 2.33††	40.78 ± 2.58††	1.60 ± 0.21††	0.56 ± 0.15††	0.57 ± 0.11††	0.29 ± 0.06††	0.24 ± 0.04††	12.61 ± 2.00††
si-OMD	185.29 ± 9.45	6.19 ± 2.16††	41.69 ± 2.12††	1.65 ± 0.27††	0.59 ± 0.19††	0.62 ± 0.10††	0.32 ± 0.07††	0.28 ± 0.04††	13.51 ± 2.83†
PHN	188.66 ± 13.41	521.75 ± 133.83**	25.71 ± 2.66**	6.25 ± 1.17**	3.96 ± 0.91**	2.10 ± 0.47**	2.18 ± 0.42**	0.42 ± 0.05**	16.87 ± 2.79**
PHN+si-OMD	183.28 ± 14.12	340.24 ± 91.47**†	28.54 ± 2.59**†	5.03 ± 0.91**	3.01 ± 0.96**	1.40 ± 0.45**	1.62 ± 0.27**†	0.36 ± 0.06**†	14.11 ± 2.87†

[Data are presented as means ± SDs; n = 8 per group. $*P < 0.05$, $**P < 0.01$ versus NC group; $^{\dagger}P < 0.05$, $^{\dagger\dagger}P < 0.01$ versus PHN group.]

OMD silencing attenuated renal podocyte injury in PHN rats

The impact of OMD silencing on renal podocyte injury was further investigated at the pathological level. As depicted in Fig. 1A-B, PHN rats exhibited typical pathological features of MN, including glomerular subepithelial dense deposits and extensive podocyte foot process fusion, evidenced by a marked increase in foot process width. Additionally, Nephrin and Podocin, key components of the podocyte slit diaphragm, showed decreased and redistributed expression in the glomeruli of PHN rats (Fig. 1C). Desmin, a well-established marker of podocyte injury, was also significantly elevated in the glomeruli of PHN rats (Fig. 1D-E). OMD silencing led to a notable attenuation of these lesions in renal podocytes, as reflected by reduced foot process width, indicative of alleviated foot process fusion (Fig. 1A-B), increased expression and normalized distribution of Nephrin and Podocin (Fig. 1C), and decreased Desmin expression in the glomeruli of the PHN+si-OMD group (Fig. 1D-E). OMD silencing did not affect the histology of normal renal tissue, as the ultrastructure of glomeruli and the expression and distribution of Nephrin, Podocin, and Desmin were consistent between the NC and si-OMD groups (Fig. 1A-E). Overall, these findings suggest that OMD silencing mitigates renal podocyte injury in PHN rats.

OMD silencing inhibited renal pyroptosis in PHN rats

The underlying mechanism of the protective effect of OMD silencing in MN was further investigated. As illustrated in Fig. 2A-B, PHN rats exhibited marked increases and activation of renal OMD, p38 MAPK, and pyroptosis, indicated by elevated expression levels of OMD, p-p38 MAPK (Thr180/Tyr182), and key pyroptosis signaling components such as NLRP3, ASC, Caspase-1, Caspase-1 p20, IL-1β, IL-18, GSDMD, and GSDMD-N in the kidney, along with increased serum levels of IL-1β and IL-18 (Fig. 2C-D). OMD silencing effectively reduced renal OMD expression in both NC and PHN rats, as demonstrated by the significantly decreased levels of OMD in the si-OMD and PHN+si-OMD groups (Fig. 2A-B). Furthermore, OMD silencing inhibited renal p38 MAPK activation and pyroptosis in PHN rats, as evidenced by reduced renal expression of p-p38 MAPK (Thr180/Tyr182) and pyroptosis markers, along with decreased serum IL-1β and IL-18 levels in the PHN+si-OMD group (Fig. 2A-D). Under physiological conditions, OMD silencing had no significant impact on p38 MAPK or pyroptosis, as no notable differences were observed in the renal expression of p38 MAPK, p-p38 MAPK (Thr180/Tyr182), or pyroptosis signaling components, nor in the serum levels of IL-1β and IL-18 between the NC and si-OMD groups (Fig. 2A-D). These results collectively demonstrate that OMD silencing effectively inhibits renal pyroptosis in PHN rats.

Discussion

The present study demonstrates that OMD silencing mitigates renal podocyte injury in MN through the inhibition of pyroptosis. The prevalence of MN is increasing rapidly[20-22]. Current MN therapies, primarily centered on cyclophosphamide and rituximab, are plagued by significant toxicities such as infection, myelosuppression, liver dysfunction, infertility, malignancy, and limited long-term efficacy[23-25]. Consequently, there is a pressing need to explore more effective treatments for MN. Pyroptosis, driven by NLRP3, plays a critical role in renal injury across various kidney diseases, including acute kidney injury (AKI), diabetic nephropathy (DN), chronic kidney disease (CKD) and ESRD[26-30], highlighting the therapeutic potential of pyroptosis inhibitors. In 2022, Wang *et al.*[6] identified the significant upregulation of pyroptosis signaling

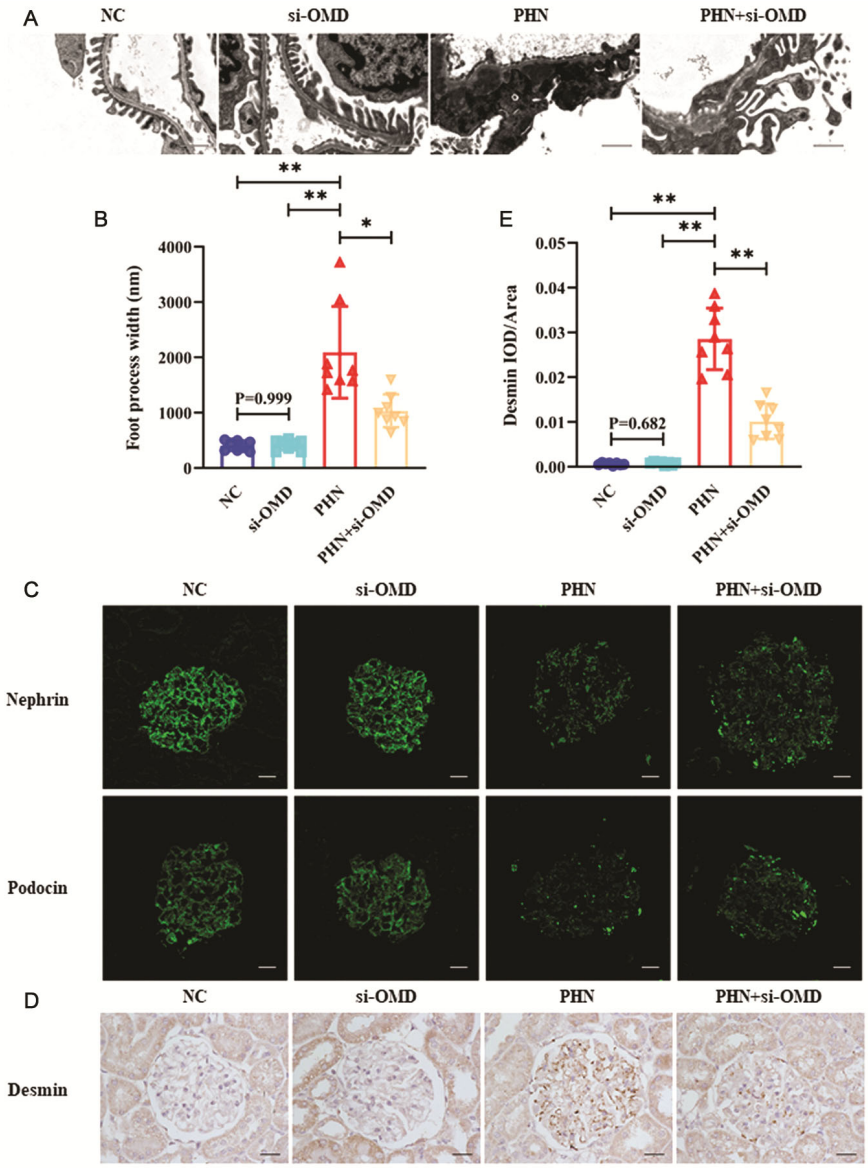

Fig. 1 — OMD silencing attenuated renal podocyte injury in PHN rats. Representative glomerular TEM images (A) and podocyte foot process width (B) for each group of rats (n = 8); scale bars = 2 μm. Representative renal immunofluorescence staining of Nephrin and Podocin (C) for each group of rats (n = 8); scale bars = 20 μm. Representative renal immunohistochemical staining of Desmin (D) and semiquantification of glomerular IOD/area (E) for each group of rats (n = 8); scale bars = 20 μm. [Data are presented as means ± SDs; $*P < 0.05$, $**P < 0.01$]

molecules—such as NLRP3, ASC, Caspase-1, IL-1β, and GSDMD—in models of complement-induced podocyte damage, PHN rat kidneys, and patients with MN, underscoring the need for discovering upstream regulators and inhibitors of pyroptosis as novel MN treatments. In our established PHN rat models, characterized by typical nephrotic syndrome and podocyte injury, the presence of intrarenal pyroptosis in MN was confirmed by the upregulation and activation of pyroptosis-related signaling molecules, including NLRP3, ASC, Caspase-1, IL-1β, IL-18, and GSDMD in the kidneys, along with increased serum levels of IL-1β and IL-18, likely originating from the kidney. Based on these observations, OMD silencing effectively alleviated nephrotic syndrome and renal podocyte injury in PHN rats by inhibiting p38 MAPK and pyroptosis. Notably, OMD silencing did not disrupt renal homeostasis, as evidenced by the absence of significant differences in renal function, histology, or pyroptosis signaling between the NC and si-OMD groups. The consistent body weight across all groups further suggests the safety of OMD

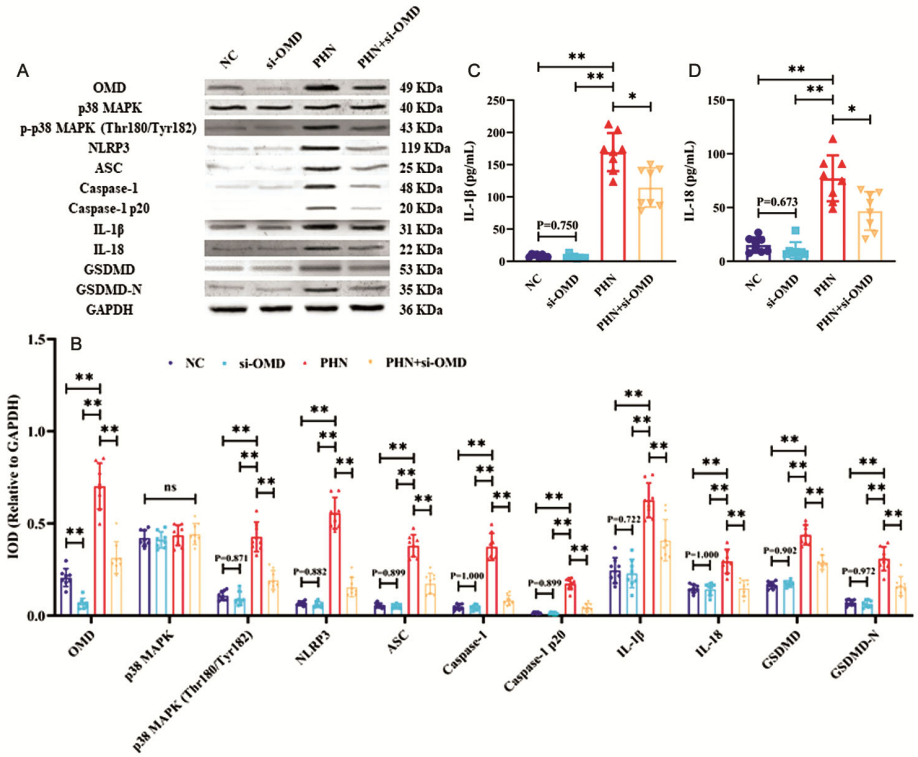

Fig. 2 — OMD silencing inhibited renal pyroptosis in PHN rats. Representative renal Western blot images of OMD, p38 MAPK, p-p38 MAPK (Thr180/Tyr182), NLRP3, ASC, Caspase-1, Caspase-1 p20, IL-1β, IL-18, GSDMD, GSDMD-N, and GAPDH (A), along with semiquantification based on IOD relative to GAPDH (B) for each group of rats (n = 8). Serum levels of IL-1β (C) and IL-18 (D) in each group of rats (n = 8). [Data are presented as means ± SDs; *$P < 0.05$, **$P < 0.01$]

inhibition in both normal and MN conditions, highlighting the potential for the clinical translation of OMD inhibitors in MN treatment.

This study further indicates that increased OMD expression and p38 MAPK activation may contribute to renal podocyte injury in MN. The inhibition of p38 MAPK and pyroptosis following OMD silencing suggests that these pathways are likely downstream of OMD. To the best of our knowledge, this is an early study to illustrate the role of OMD in kidney diseases and to propose a potential link between OMD and pyroptosis. Previous research has implicated OMD in the pathogenesis of keloids, where it promotes hyperproliferation, migration, and excessive extracellular matrix synthesis in keloid-derived fibroblasts *via* p38 MAPK regulation[11]. Additionally, OMD has been recognized for its physiological roles, such as facilitating osteogenesis and inhibiting apoptosis in human dental pulp stem cells[12,31]. p38 MAPK, a major branch of the MAPK signaling cascade[32,33], is known to play a critical role in the progression of various kidney diseases, including AKI, CKD, DN and lupus nephritis[34-38]. Our findings align with previous studies showing that p38 MAPK activation, potentially regulated by OMD, is associated with MN-related podocyte injury, similar to the activation of p38 MAPK seen in C5b-9 or secretory phospholipase A2 group IB-induced podocyte injury model of MN[39,40]. This underscores the detrimental effects of excessive p38 MAPK activation in MN. Interestingly, OMD silencing did not affect inactivated p38 MAPK under physiological conditions, suggesting that additional signaling pathways may be involved in or modulate OMD's regulation of p38 MAPK. Further research is required to fully elucidate the regulatory network of OMD in the kidney.

Conclusion

We identify OMD as a key regulator of pyroptosis in MN. Its silencing alleviates renal podocyte injury by suppressing the p38 MAPK axis and subsequent pyroptosis. These results highlight OMD inhibition as a promising therapeutic approach for MN.

Ethical statement

The animal experimental protocols of the study were approved by the Experimental Animal Ethics Committee of Jiangnan University (Approval number: JN.No20231215S0400801-612).

Acknowledgements

This work was supported by the Scientific Research Program of the Wuxi Commission of Health (Q202308); Wuxi Science and Technology Development Fund "Light of the Taihu Lake" Scientific and Technological Project (K20241017) and the Wuxi Translational Medicine Research Institute (project number: LCYJ202340).

Conflict of interest

The authors declare no conflicts of interest.

References

1 Claudio P. Primary membranous nephropathy an endless story. *J Nephrol*, 36 (2023) 563.
2 Kistler AD & Salant DJ. Complement activation and effector pathways in membranous nephropathy. *Kidney Int*, 105 (2024) 473.
3 Ponticelli C. Membranous Nephropathy. *J Clin Med*, 14 (2025).
4 Sanz AB, Sanchez-Niño MD, Ramos AM & Ortiz A. Regulated cell death pathways in kidney disease. *Nat Rev Nephrol*, 19 (2023) 281.
5 Gao H, Xie T, Li Y, Xu Z, Song Z, Yu H , Zhou H, Li W, Yun C, Guan B, Luan S &Yin L .Role of gasdermins in chronic kidney disease. *Front Immunol*, 16 (2025) 1557707.
6 Wang H, Lv D, Jiang S, Hou Q, Zhang L, Li S , Zhu X, Xu X, Wen J, Zeng C, Zhang M, Yang F, Chen Z, Zheng C, Li J, Zen K, Liu Z & Li L. Complement induces podocyte pyroptosis in membranous nephropathy by mediating mitochondrial dysfunction. *Cell Death Dis*, 13 (2022) 281.
7 Lv D, Chu L, Du Y, Li C, Bao N, Su Y, Wang G, Zheng Y& Yu Y. Sulforaphane alleviates membranous nephropathy by inhibiting oxidative stress-associated podocyte pyroptosis. *Iran J Basic Med Sci*, 28 (2025) 237.
8 Guo Y, Min J, Chang B, Chen Z & Chen W. Exploring the Role of TRAF6-TAK1 Pathway in Podocyte Pyroptosis and Its Implications for Primary Membranous Nephropathy Therapy. *Inflammation* (2025).
9 Wendel M, Sommarin Y & Heinegård D. Bone matrix proteins: isolation and characterization of a novel cell-binding keratan sulfate proteoglycan (osteoadherin) from bovine bone. *J Cell Biol*, 141 (1998) 839.
10 Hamaya E, Fujisawa T & Tamura M. Osteoadherin serves roles in the regulation of apoptosis and growth in MC3T3-E1 osteoblast cells. *Int J Mol Med*, 44 (2019) 2336.
11 Li Q, Chen H, Liu Y & Bi J. Osteomodulin contributes to keloid development by regulating p38 MAPK signaling. *J Dermatol*, 50 (2023) 895.
12 Dong T, Lin WZ, Zhu XH, Yuan KY, Hou LL & Huang ZW. Osteomodulin protects dental pulp stem cells from cisplatin-induced apoptosis in vitro. *Stem Cell Rev Rep*, 19 (2023) 188.
13 Cuadrado A & Nebreda AR. Mechanisms and functions of p38 MAPK signalling. *Biochem J*, 429 (2010) 403.
14 Wang Y, Yu Y, Yu W, Bian X & Gong L. IL-35 inhibits cell pyroptosis and attenuates cell injury in TNF-α-induced bronchial epithelial cells via p38 MAPK signaling pathway. *Bioengineered*, 13 (2022) 1758.
15 Zhu QQ, Zhang Y, Cui L, Ma L & Sun KW. Downregulation of AQP9 Ameliorates NLRP3 Inflammasome-Dependent Inflammation and Pyroptosis in Crohn's Disease by Inhibiting the p38 MAPK Signaling Pathway. *Mol Biotechnol* (2025).
16 Hayashi N, Kumar S, Trivin Avillach C, Fan X, Stoddard SV, Akai R , Fujimoto K , Iwawaki T , Yokoyama H, Furuichi K, Beck LH Jr. Characterization of FAM114A1: a novel podocyte cytoskeleton-associated protein upregulated in glomerular injury. *Am J Physiol Renal Physiol*, 328 (2025) F289.
17 Pan Y, Chen S, Wu L, Xing C, Mao H, Liang H & Yuan Y. Animal models of membranous nephropathy: more choices and higher similarity. *Front Immunol*, 15 (2024) 1412826.
18 Salant DJ & Cybulsky AV. Experimental glomerulonephritis. *Methods Enzymol*, 162 (1988) 421.
19 White KE & Bilous RW. Estimation of podocyte number a comparison of methods. *Kidney Int*, 66 (2004) 663.
20 Tang L, Yao J, Kong X, Sun Q, Wang Z, Zhang Y , Wang P , Liu Y , Li W , Cui M , Zhen J & Xu D. Increasing prevalence of membranous nephropathy in patients with primary glomerular diseases: A cross-sectional study in China. *Nephrology (Carlton)*, 22 (2017) 168.
21 Li J, Cui Z, Long J, Huang W, Wang J, Zhang H , Wang H, Zhang L, Ronco P&Zhao MH . Primary glomerular nephropathy among hospitalized patients in a national database in China. *Nephrol Dial Transplant*, 33 (2018) 2173.
22 Hou JH, Zhu HX, Zhou ML, Le WB, Zeng CH, Liang SS, Xu F, Liang DD, Shao SJ, Liu Y, Liu ZH. Changes in the Spectrum of Kidney Diseases: An Analysis of 40,759 Biopsy-Proven Cases from 2003 to 2014 in China. *Kidney Dis (Basel)*, 4 (2018) 10.
23 Shah M, DeLaat A & Cavanaugh C. Treatment of membranous nephropathy: Perspectives on current and future therapies. *Front Nephrol*, 3 (2023) 1110355.
24 Gauckler P, Shin JI, Alberici F, Audard V, Bruchfeld A, Busch M , Cheung CK , Crnogorac M , Delbarba E , Eller K, Faguer S, Galesic K, Griffin S, van den Hoogen MWF, Hrušková Z, Jeyabalan A, Karras 2 A, King C, KohliHS, Mayer G, Maas R, Muto M, Moiseev S, Odler B, Pepper RJ, Quintana LF, Radhakrishnan J, Ramachandran R, Salama AD, Schönermarck U, Segelmark M, Smith L, Tesař V, Wetzels J, Willcocks L, Windpessl M, Zand L, Zonozi R & Kronbichler. Rituximab in Membranous Nephropathy. *Kidney Int Rep*, 6 (2021) 881.
25 Efe O, So PNH, Anandh U, Lerma EV & Wiegley N. An Updated Review of Membranous Nephropathy. *Indian J Nephrol*, 34 (2024) 105.
26 Li C, Yang H, Wu Y, Zhou M, Luo H, Yuan P , Shen F. Carnosol alleviates cisplatin-induced acute kidney injury by regulating apoptosis and pyroptosis. *Cell Biol Int*, 49 (2025) 101.
27 Wang X, Wu S, Jiang Y, Yuan Z, Liu J, Jing S, Liu J, Sun J, Wang C, Wang D& Li H. Anwulignan alleviates IRI by the activation of Nrf2/HO-1 signaling pathway and inhibiting NLRP3-caspase-1-GSDMD-mediated pyroptosis in rats. *Tissue Cell*, 93 (2025) 102775.
28 Hu X, Wang J, Jiang L, Liu X, Ge Q, Wang Q , Qi X &Wu Y. Rutaecarpine protects podocytes in diabetic kidney disease by targeting VEGFR2/NLRP3-mediated pyroptosis. *Int Immunopharmacol*, 130 (2024) 111790.

29 Cheng Y, Lu Z, Mao T, Song Y, Qu Y, Chen X , Chen K , Liu K & Zhang C. Magnoflorine Ameliorates Chronic Kidney Disease in High-Fat and High-Fructose-Fed Mice by Promoting Parkin/PINK1-Dependent Mitophagy to Inhibit NLRP3/Caspase-1-Mediated Pyroptosis. *J Agric Food Chem*, 72 (2024) 12775.

30 Zhang X & Yang B. The serum levels of gasdermin D in uremic patients and its relationship with the prognosis: a prospective observational cohort study. *Ren Fail*, 46 (2024) 2312534.

31 Lin W, Zhu X, Gao L, Mao M, Gao D & Huang Z. Osteomodulin positively regulates osteogenesis through interaction with BMP2. *Cell Death Dis*, 12 (2021) 147.

32 Goncalves IL, Tal S, Barki-Harrington L & Sapir A. Conserved statin-mediated activation of the p38-MAPK pathway protects Caenorhabditis elegans from the cholesterol-independent effects of statins. *Mol Metab*, 39 (2020) 101003.

33 Du G, Zheng K, Sun C, Sun M, Pan J, Meng D, Guan W& Zhao H. The relationship mammalian p38 with human health and its homolog Hog1 in response to environmental stresses in Saccharomyces cerevisiae. *Front Cell Dev Biol*, 13 (2025) 1522294.

34 Xiang H, Li Z, Li Y, Zheng J, Dou M, Xue W& Wu X. Dual-specificity phosphatase 26 protects against kidney injury caused by ischaemia-reperfusion through restraint of TAK1 JNK/p38-mediated apoptosis and inflammation of renal tubular epithelial cells. *Toxicol Appl Pharmacol*, 487 (2024) 116954.

35 Wang N & Zhang C. Oxidative Stress: A Culprit in the Progression of Diabetic Kidney Disease. *Antioxidants (Basel)*, 13 (2024).

36 Lai Y, Tang H, Zhang X, Zhou Z, Zhou M, Hu Z, Zhu F, Zhang L& Nie J. Trimethylamine-N-Oxide Aggravates Kidney Injury via Activation of p38/MAPK Signaling and Upregulation of HuR. *Kidney Blood Press Res*, 47 (2022) 61.

37 Lee SM, Lee S, Kim KH, Kim D, Park SJ, Kim KH , Lee S, Bae E, Yoo KD, Lee JW, Park JY, Kim YS, Cha RH & Yang SH . Field direction of static magnetic fields influences kidney fibrosis progression through MAPK signaling and cell cycle alteration. *Sci Rep*, 15 (2025) 24841.

38 Qi H, Xu L & Liu Q. Knockdown of DEC2 expression inhibits the proliferation of mesangial cells through suppressed glycolysis and p38 MAPK/Erk pathway in lupus nephritis. *Mol Med*, 29 (2023) 99.

39 Yang L, Wu Y, Lin S, Dai B, Chen H, Tao X, Li G, Wan J& Pan Y. sPLA2-IB and PLA2R mediate insufficient autophagy and contribute to podocyte injury in idiopathic membranous nephropathy by activation of the p38MAPK/mTOR/ULK1(ser757) signaling pathway. *FASEB J*, 35 (2021) e21170.

40 Hong T, Cui LK, Wen J, Zhang MH & Fan JM. [Cordycepin protects podocytes from injury mediated by complements complex C5b-9]. *Sichuan Da Xue Xue Bao Yi Xue Ban*, 46 (2015) 173.